Frequency bandwidth enhancement using 3D layered reflectivity inversion

Rick Walia, N. Chaminda Sandanayake, Michael Koop, CGG Canada Services Ltd.*
Andrew Williamson, Karin Michel, EnCana Corporation

Summary

A new methodology for frequency bandwidth enhancement using 3D layered reflectivity inversion is presented in this paper. The inversion is used to obtain layered reflectivity and then band-limited to the outer bounds of the input seismic. The 3D-reflectivity inversion starts with a thin layer model based on the geological picks following the structural and stratigraphic trends. The initial thickness of the thin layers is determined by the frequency bandwidth of the seismic data, and the inversion process orients them conformable to stratigraphic layers in the subsurface. The thickness and impedance of each layer (and hence interface reflection coefficient) is perturbed and the corresponding modelled synthetic is compared to the seismic data in a volumetric fashion to minimise the misfit (Walia, 2001). This contributes to the removal of tuning effects and provides a reflectivity sequence with a much higher frequency bandwidth than the seismic data. Subsequently, the reflection series is band-limited to obtain higher resolution seismic data. The limits of bandwidth enhancement is selected by correlating the enhanced seismic to well logs and VSPs.

The comparison of seismic profiles, attribute maps and correlation with well data presented in this paper confirm that this process has resolved real seismic events. This resulted in confident picking of top and base of individual sand units, consequently providing better maps of the reservoir sands.

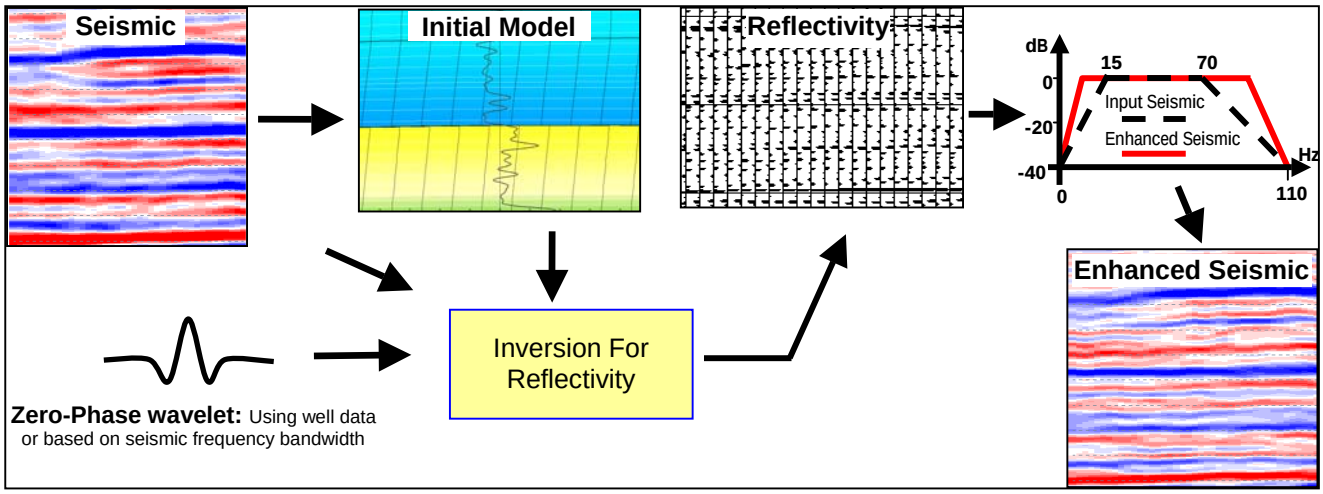

Fig. 1: Frequency bandwidth enhancement workflow.

Application to Seismic Data

Rigorous study of this technique on several 3D data volumes from the North Sea and Ecuador's Oriente Basin have produced very encouraging results in terms of resolving Top/Base of producing thin sands, improving structural features and complex-fault definition. Fig. 1 shows a simple workflow of the methodology. An initial model, based on the main geological horizons and log data, is input to the inversion process. The inversion process describes the existing zero-phase 3D volume by a discrete number of thin (half of time-thickness of the input wavelet) layers (Ricker, 1953). Each layer consists of two parameters, the time thickness and initial impedance and hence reflection coefficient value at the interface of every bin location. During the inversion process both the parameters are perturbed within pre-defined constraints. Convergence to the final solution is achieved using a full 3D algorithm based on simulated annealing. The resulting layered structure provides an effective resolution of typically an eighth of the wavelength (Gluck et al, 1997; Widess, 1973). The data reduction implicit in the layer definition makes this algorithm extremely robust to noise.

This inverted reflectivity is then band-limited such that the enhanced seismic has a broader frequency bandwidth than the input seismic. Extensive QCs are carried out to estimate the optimum frequency bandwidth so that only genuine frequencies corresponding to the signal are retained. Fig. 2 shows a comparison of the seismic data from the Oriente Basin before and after

this process. Unambiguous resolution of the top and base of the reservoir zone is demonstrated and can be mapped throughout the 3D.

Filter panels of the seismic data before and after the frequency enhancement process are shown in Fig. 3. It can be seen that the continuity and the signal-to-noise have been improved by this process, as shown in the lower (black box) as well as the higher frequency bands (green box). The ringing in the 70 - 100 Hz frequency panels in the input seismic has now been replaced with true high frequency events representing distinct thin geological sequences. As shown by the filter panels, the seismic data input to the process was already spectrally whitened to its maximum using conventional methods (Knapp, 1990; Okoya, 1995) and therefore only frequencies < 14 Hz and > 60 Hz were enhanced by this process.

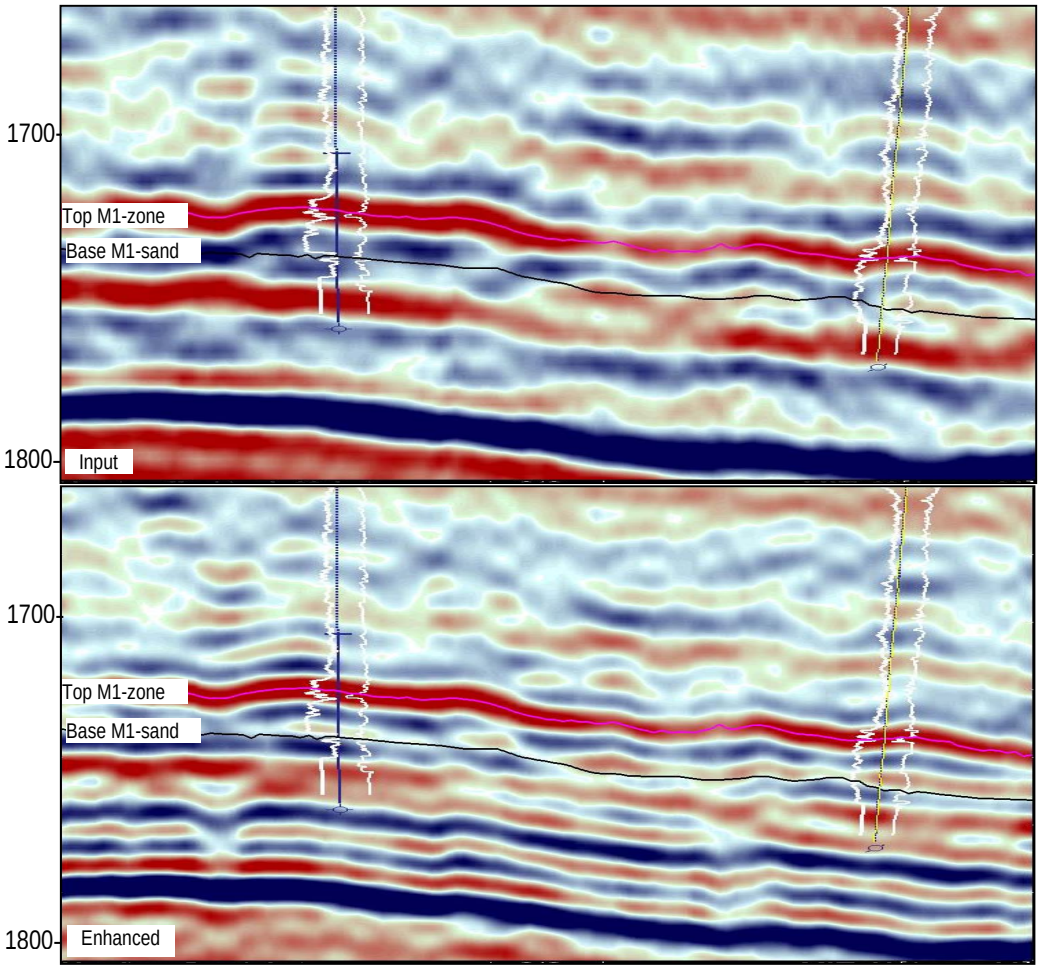

Fig. 2: Comparison of original seismic data before and after the enhancement process. The purple horizon is M1-zone top and the black horizon is the base of the sand. It is clear that the top and the base of the zone can be picked unambiguously on the enhanced section. Gamma ray (left) and sonic (right) logs are displayed at the wells.

A synthetic seismogram at the well TU–1 was computed using a zero-phase wavelet (2-8-85-100 Hz) (Fig. 4) to compare the results of this process. The match between the seismic and the synthetic is reasonably good, the enhanced seismic shows further improvement particularly for a few events (note the red boxes in Fig. 4). This demonstrates that this process has resolved the real seismic events.

To assess the bandwidth improvement of the enhanced seismic for interpretation, the Dip, Central Frequency, and Amplitude maps at the reservoir are compared before and after the enhancement process (Fig. 5, 6 & 7). Comparison of dip attribute maps (Fig. 5) clearly shows that geological features, particularly faults and fault splays are better resolved on the maps produced from frequency enhanced seismic volume.

The central frequency map calculated in a window centred at the M1-zone top from the input and the enhanced seismic is compared in Fig. 6. The orientation of the higher frequencies is distinct and the histograms suggest that the dominant frequency

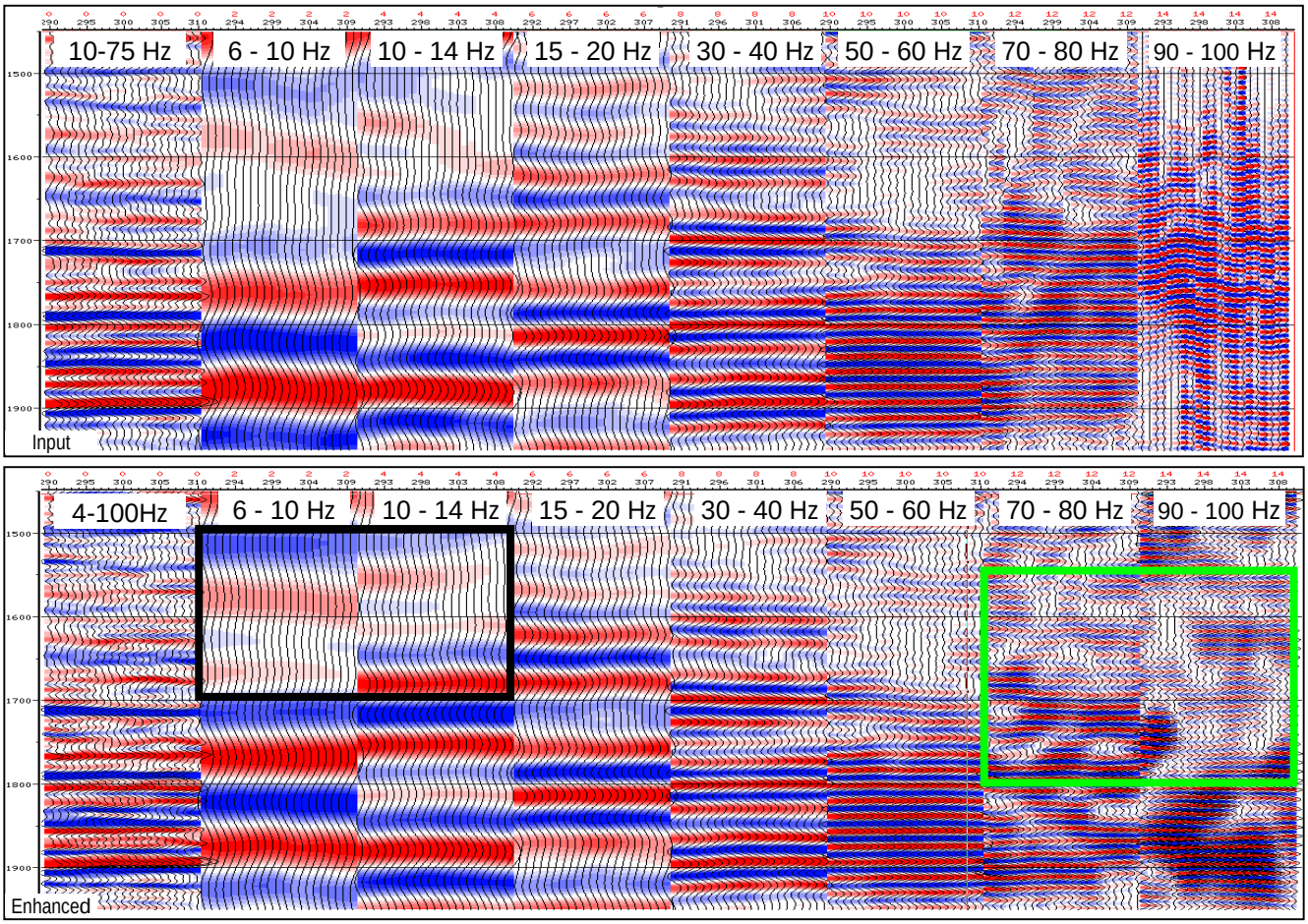

Fig. 3: Filter panels of the seismic data before and after the frequency enhancement process. It is clear from the comparison that continuity and signal-to-noise have been improved by this process in the lower (black box) as well as the higher (green box) frequency bands. The ringing in the 70 - 100 Hz frequency panels in the input seismic have now been replaced with true high frequency events representing distinct thin geological sequences.

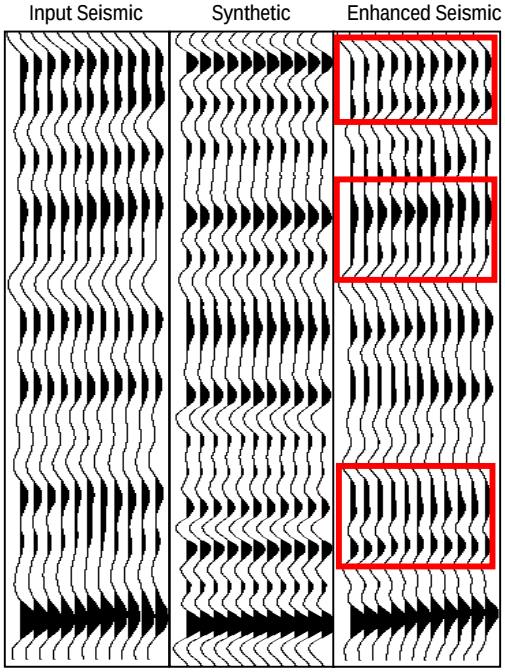

has increased from 46 Hz to about 56 Hz. Amplitude map (Fig. 7) from enhanced seismic exhibits greater details of stratigraphic features as shown.

Conclusions

We demonstrated that the methodology described in this paper has successfully enhanced the frequency bandwidth of the input data, which was not possible to achieve by conventional processing methods. The comparison of seismic profiles and attribute maps before and after the process, and an improved correlation with well data confirm that the frequency bandwidth enhancement process has resolved real seismic events. This has resulted in confident picking of top and base of individual sand units consequently providing better maps of the reservoir sands.

Acknowledgements

The authors thank EnCana Corporation and CGG Canada Services Ltd. for their approval to publish this work.

Fig. 4: Seismic traces before and after the enhancement process are compared with the synthetics at well TU-1. As shown (red boxes), the enhanced seismic matches very well with the synthetics. This shows that real seismic events have been resolved.

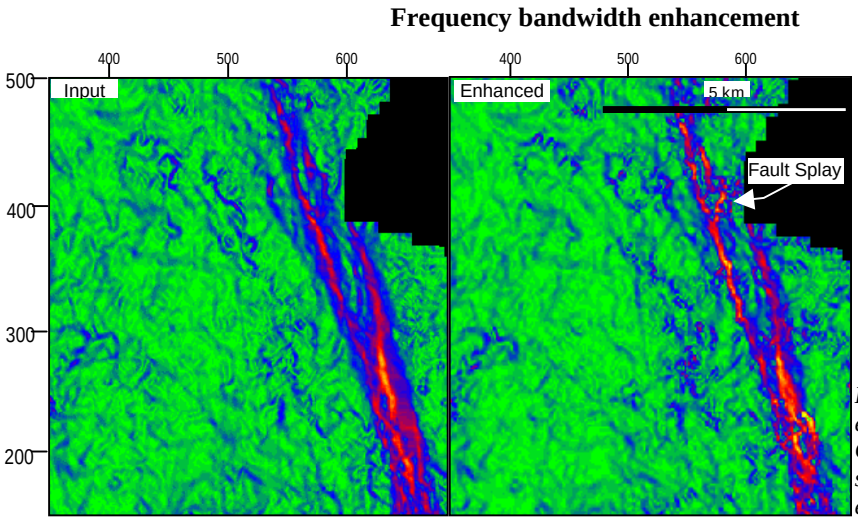

Fig. 5: Dip attribute map of input and enhanced seismic for M1-zone top. Geological features, particularly fault splays are better resolved on the enhanced seismic.

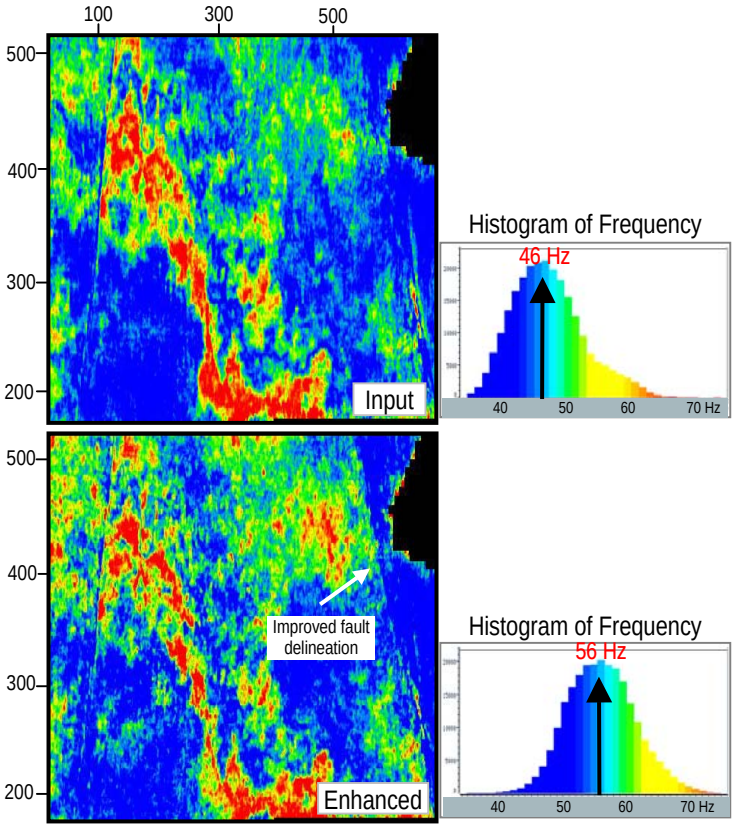

Fig. 6: Central frequency map of input and enhanced seismic at M1-zone top. The orientation of the higher frequencies are focussed and represent features consistent with the depositional environment.

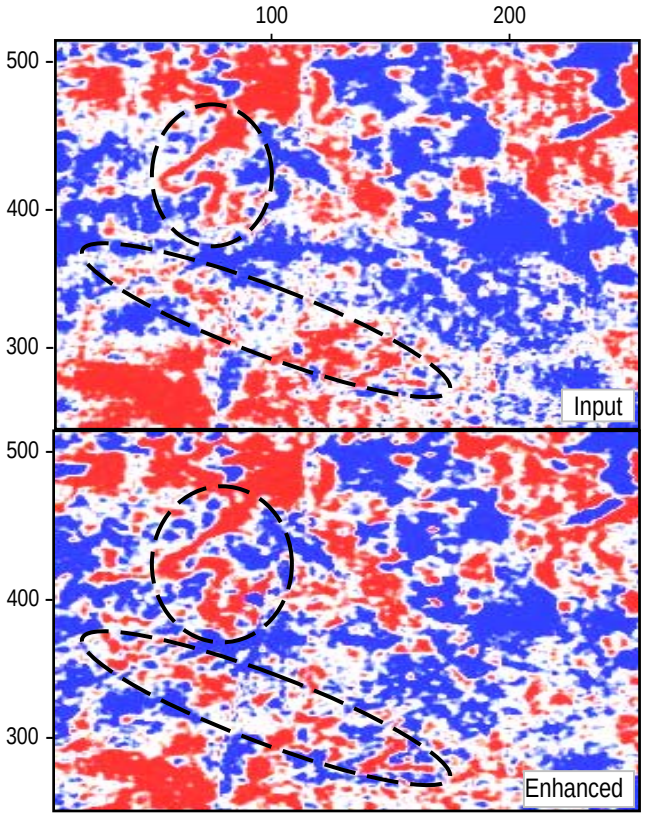

Fig. 7: Amplitude map of input and enhanced seismic below 14ms M1-zone top. Enhanced slice exhibits greater details of stratigraphic features as shown.

References

Gluck, S., Juve, E., and Lafet, Y., 1997, High-resolution impedance layering through 3-D stratigraphic inversion of poststack seismic data: The Leading Edge, **16**, pp1309-1315

Knapp, R. W., 1990, Vertical resolution of thick beds, thin beds, and thin-bed cyclothems: Geophysics, **55**, 1183-1190.

Okoya, D.A., 1995, Spectral properties of the earth's contribution to seismic resolution: Geophysics, **60**, 241-251.

Ricker, N., 1953, Wavelet contraction, wavelet expansion and the control of seismic resolution: Geophysics, **18**, 769-792.

Walia, R., 2001, Stratigraphic inversion of a Wabamun carbonate play – parkland field: The CSEG Recorder, **26**, 26-35.

Widess, M. B., 1973, How thin is a thin bed?: Geophysics, **38**, 1176-1180.